Molecular Study of Malignant Gliomas Treated with Epidermal Growth Factor Receptor Inhibitors: Tissue Analysis from North American Brain Tumor Consortium Trials 01-03 and 00-01

Andrew B. Lassman,[1] Michael R. Rossi,[5] Jeffrey R. Razier,[6] Lauren E. Abrey,[1] Frank S. Lieberman,[7] Chelsea N. Grefe,[2] Kathleen Lamborn,[8] William Pao,[2,3] Alan H. Shih,[2] John G. Kuhn,[9] Richard Wilson,[10] Norma J. Nowak,[5] John K. Cowell,[5] Lisa M. DeAngelis,[1] Patrick Wen,[11] Mark R. Gilbert,[12] Susan Chang,[8] W.A. Yung,[12] Michael Prados,[8] and Eric C. Holland[1,2,4]

Abstract

Purpose: We investigated the molecular effect of the epidermal growth factor receptor (EGFR) inhibitors erlotinib and gefitinib *in vivo* on all available tumors from patients treated on North American Brain Tumor Consortium trials 01-03 and 00-01 for recurrent or progressive malignant glioma.

Experimental Design: EGFR expression and signaling during treatment with erlotinib or gefitinib were analyzed by Western blot and compared with pre – erlotinib/gefitinib – exposed tissue or unexposed controls. Tumors were also analyzed for *EGFR* mutations and for other genomic abnormalities by array-based comparative genomic hybridization. Clinical data were used to associate molecular features with tumor sensitivity to erlotinib or gefitinib.

Results: Erlotinib and gefitinib did not markedly affect EGFR activity *in vivo*. No lung signature mutations of EGFR exons 18 to 21 were observed. There was no clear association between erlotinib/gefitinib sensitivity and deletion or amplification events on array-based comparative genomic hybridization analysis, although novel genomic changes were identified.

Conclusions: As erlotinib and gefitinib were generally ineffective at markedly inhibiting EGFR phosphorylation in these tumors, other assays may be needed to detect molecular effects. Additionally, the mechanism of erlotinib/gefitinib sensitivity likely differs between brain and lung tumors. Finally, novel genomic changes, including deletions of chromosomes 6, 21, and 22, represent new targets for further research.

The prognosis for patients with high-grade gliomas is poor, with a median survival of 2 to 5 years for anaplastic astrocytomas and 1 year for glioblastomas (1). Unfortunately, glioblastomas are the most common as well as most aggressive subtype (1). New therapies are needed, and small-molecule inhibitors targeting specific molecular abnormalities important in glioma biology may provide benefit (2).

Several types of abnormalities of epidermal growth factor receptor (EGFR), a receptor tyrosine kinase, contribute to the growth and proliferation of tumor cells in the majority of glioblastomas, including *EGFR* gene amplification, protein overexpression, and constitutively activating mutations (3 – 9). Normally, EGF and other ligands activate the EGFR, causing dimerization/oligomerization and activation of intrinsic tyrosine kinase activity in the cytosolic domain of the receptor (Fig. 1A; ref. 10). When activated, the receptor both autophosphorylates and initiates downstream signaling through the RAS-MAPK and phosphatidylinositol 3-kinase (PI3K)/AKT signal

Authors' Affiliations: Departments of [1]Neurology, [2]Cancer Biology and Genetics, [3]Medicine, and [4]Surgery (Neurosurgery), Memorial Sloan Kettering Cancer Center, New York, New York; [5]Roswell Park Cancer Institute, Buffalo, New York; [6]Department of Neurology, Northwestern University, Feinberg School of Medicine, Chicago, Illinois; [7]University of Pittsburgh Medical Center Cancer Pavilion, Pittsburgh, Pennsylvania; [8]Neuro-Oncology Services, University of California-San Francisco, San Francisco, California; [9]University of Texas Health Science Center, San Antonio, Texas; [10]Genome Sequencing Center, Washington University School of Medicine, St. Louis, Missouri; [11]Department of Neurology, Dana-Farber Cancer Institute, Boston, Massachusetts; and [12]Department of Neuro-Oncology, University of Texas M.D. Anderson Cancer Center, Houston, Texas

Received 2/25/05; revised 6/24/05; accepted 8/9/05.

Grant support: NIH/National Cancer Institute grants T32 CA009512 (A.B. Lassman and W. Pao), 5-U01CA62399-09 (A.B. Lassman, J.R. Raizer, L.E. Abrey, L.M. DeAngelis, and E.C. Holland), R21 CA104504 (M.R. Rossi, N.J. Nowak, and J.K. Cowell), CA62426 (J. Kuhn), U01CA62407-08 (P. Wen), CA62412 and CA62422 (K. Lamborn, S. Chang, and M. Prados), CA62412 (M.R. Gilbert and W.A. Yung), and RO1 CA099489, RO1 CA100688, and UO1 CA894314-1 (A.B. Lassman, C.N. Grefe, A.H. Shih, and E.C. Holland); American Brain Tumor Association (A.B. Lassman); Chest and LUNGevity Foundations of the American College of Chest Physicians and an anonymous donor (W. Pao); and Bressler, Seroussi, and Kirby Foundations (E.C. Holland).

The costs of publication of this article were defrayed in part by the payment of page charges. This article must therefore be hereby marked *advertisement* in accordance with 18 U.S.C. Section 1734 solely to indicate this fact.

Note: Supplementary data for this article are available at Clinical Cancer Research Online (http://clincancerres.aacrjournals.org/).

Requests for reprints: Andrew B. Lassman, Department of Neurology, Memorial Sloan Kettering Cancer Center, 1275 York Avenue, New York, NY 10021. Phone: 212-639-6037; Fax: 212-717-3519; E-mail: lassmana@mskcc.org.

doi:10.1158/1078-0432.CCR-05-0421

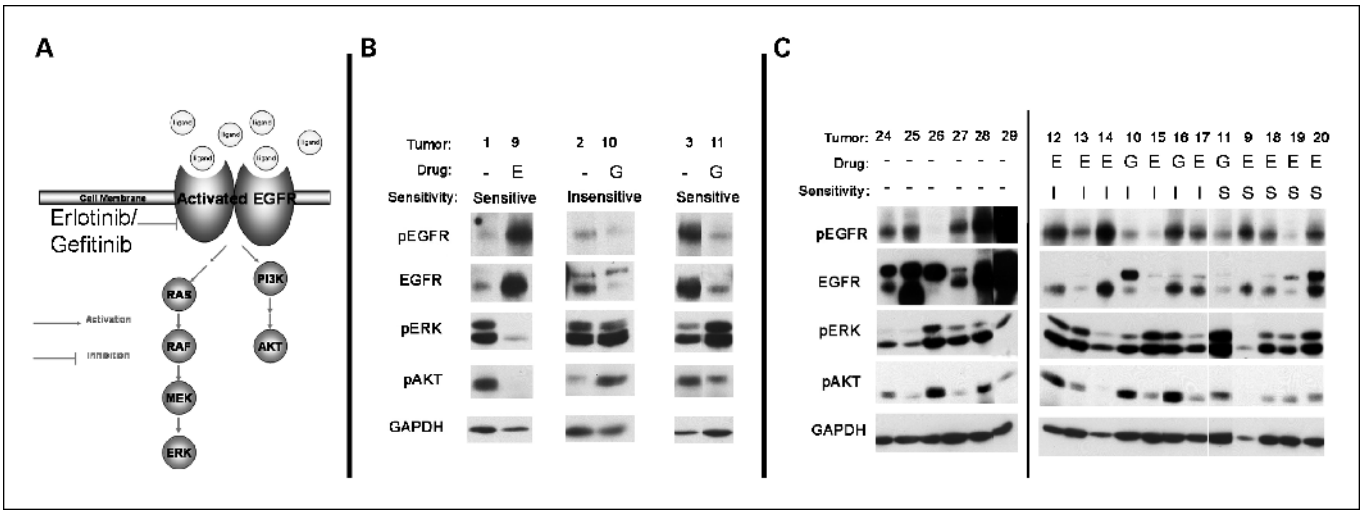

Fig. 1. *A,* normally, ligands (such as EGF and transforming growth factor-α) stimulate EGFR activation, which initiates signal transduction through the RAS/MAPK and the PI3K/AKT cascades. *B,* comparison of tumors resected before (*1-3*) or during (*9-11*) erlotinib (*E*)/gefitinib (*G*) from a three patients. *C,* malignant gliomas resected during treatment with erlotinib/gefitinib (*9-20*) were compared with erlotinib/gefitinib unexposed control gliomas (*24-29*). The range of pEGFR, pERK, and pAKT in tumors during erlotinib/gefitinib treatment did not differ substantially from the range observed in controls. There was no consistent pattern of difference between tumors that were sensitive (*S*) or insensitive (*I*) to erlotinib/gefitinib.

transduction cascades. Activation of EGFR, RAS, and AKT can be detected by analysis of tumor tissue for pEGFR, pERK, and pAKT levels with commercially available antibodies.

The EGFR inhibitors erlotinib (OSI774, Tarceva) and gefitinib (ZD1839, Iressa) are currently under evaluation in clinical trials for gliomas. Seeking to determine whether erlotinib or gefitinib therapy affects EGFR signaling in malignant gliomas *in vivo* and whether observed effects determined clinical response, we analyzed all available surgically resected malignant glioma tissue from patients who were treated with erlotinib or gefitinib through two multi-institution clinical trials. We also analyzed the available tumors for mutations of the *EGFR* gene and for other genomic alterations beyond EGFR. Although we did not identify consistent inhibition of EGFR signaling by erlotinib or gefitinib, several new genomic abnormalities were identified as common to malignant gliomas and worthy of further study.

Materials and Methods

Tissue. Patients with recurrent or progressive malignant gliomas were treated with erlotinib through North American Brain Tumor Consortium (NABTC) multicenter phase I/II clinical trial 01-03 or with gefitinib through NABTC trial 00-01. Treatment and correlative analyses were approved by the institutional review board at each center and performed with patient's informed consent. Patients received daily erlotinib or gefitinib as monotherapy and were followed clinically and radiographically with brain imaging (magnetic resonance imaging or computed tomography scans) every 8 weeks thereafter until tumor progression or death. When surgical resection was medically indicated at the time of enrollment for tumor recurrence or progression (also called the surgical arm of the trials), patients received 150 mg p.o. erlotinib or 500 mg p.o. gefitinib daily for 1 week preoperatively, underwent resection, and then restarted daily erlotinib or gefitinib following recovery from surgery. These specimens were analyzed to determine the effect of erlotinib or gefitinib on EGFR signaling at the molecular level *in vivo* and to determine if molecular effects were associated with clinical response.

Twenty-one malignant gliomas from 18 patients treated with erlotinib or gefitinib were available for molecular analysis (Table 1, tumors 1-21). Criteria for clinical evaluation and final clinical results (overall survival, progression-free survival, etc.) will be reported separately for these and other patients who participated in NABTC trials 01-03 (11) or 00-01 (12). The results reported here are restricted to molecular analysis, and for the purpose of analyzing the biological activity of erlotinib/gefitinib therapy, the following criteria were applied. Ten patients were considered to have erlotinib/gefitinib–insensitive tumors because of radiographically progressive disease (>25% growth; ref. 13) or because of clinical progression within the first 8 weeks of therapy. One patient was considered to have a sensitive tumor because a complete radiographic response (13) was observed, independently confirmed on central review, which was sustained for at least 22 months. Six patients with radiographically stable disease (between 50% reduction and 25% growth; ref. 13) after 8 weeks of treatment were considered to have erlotinib/gefitinib–sensitive tumors because all patients had radiographically enlarging tumors when erlotinib was started; however, it should be noted that the stable responses were not sustained and progressive tumor growth was observed between 8 and 24 weeks after starting erlotinib in all of these cases. Finally, one patient was considered to have a sensitive tumor because of a mixed radiographic response and another because of histologically proven disease control. In sum, there were 11 insensitive tumors and 10 sensitive tumors resected from 18 patients.

Among these 21 specimens, there were 12 resected from patients during erlotinib or gefitinib treatment (Table 1, tumors 9-20). In three of these (tumors 9-11), tissue was also available from the same patients from prior excisions before treatment with an EGFR inhibitor (tumors 1-3), and direct comparison of the pretreatment and during-treatment specimens was done. In the other nine specimens (12–20), pretreatment tissue was unavailable for comparison; therefore, we compared these tumors indirectly with 12 controls of matched histology (tumors 22-33) banked from patients who did not receive erlotinib, gefitinib, or other receptor tyrosine kinase inhibitors.

Western blots. Tumors that were flash frozen in liquid nitrogen immediately following surgical resection and stored at −80°C were ground into fine powder in liquid nitrogen and dissolved in T-PER buffer (Pierce, Rockford, IL) containing EDTA-free Complete protease inhibitor cocktail (Roche, Indianapolis, IN) and the phosphatase inhibitors $NaVO_3$ (1 mmol/L; pH 10) and NaF (30 mmol/L). Protein concentrations were determined by absorption at 595 nm of diluted protein extract (Bio-Rad, Hercules, CA) relative to bovine

Table 1. Features of available tumors and analyses done

Tumor	Timing of tumor resection relative to treatment with gefitinib/erlotinib	Histology	Treated with erlotinib (E), gefitinib (G), or neither (N)	Erlotinib/gefitinib sensitive (S), insensitive (I), or not applicable (NA)	EGFR activity assayed	*EGFR* sequencing	*EGFR* amplification
1	Before	Glioblastoma	E	S	Yes	Wild-type	Marginal gain
2	Before	Glioblastoma	G	I	Yes	Wild-type	1+ *EGFR*
3	Before	Anaplastic astrocytoma	G	S	Yes	ND	ND
4	Before	Glioblastoma	E	I	Yes	Wild-type	6+ *EGFR*
5	Before	Glioblastoma	E	I	Yes	Wild-type	Marginal gain
6	Before	Anaplastic astrocytoma	E	S	No	Exons 18-21 wild-type (other exons failed)	Failed
7	Before	Anaplastic astrocytoma	E	S	Yes	Wild-type	None
8	Before	Anaplastic mixed glioma	E	S	Yes	Exon 6, heterozygous C219Y	6+ *EGFR*
9	During	Glioblastoma	E	S	Yes	Wild-type	None
10	During	Glioblastoma	G	I	Yes	Wild-type	1+ *EGFR*
11	During	Anaplastic astrocytoma	G	S	Yes	ND	ND
12	During	Glioblastoma	E	I	Yes	ND	ND
13	During	Glioblastoma	E	I	Yes	Exon 13, heterozygous R521K	Marginal gain
14	During	Glioblastoma	E	I	Yes	Exon 13, heterozygous R521K	Failed
15	During	Glioblastoma	E	I	Yes	Exon 13, homozygous R521K	1+ *EGFR*
16	During	Glioblastoma	G	I	Yes	ND	ND
17	During	Anaplastic mixed glioma	E	I	Yes	Wild-type	Marginal gain
18	During	Glioblastoma	E	S	Yes	ND	ND
19	During	Glioblastoma	E	S	Yes	ND	ND
20	During	Glioblastoma	E	S	Yes	ND	ND
21	3 months later	Glioblastoma	E	I	No	Exon 17, heterozygous R675Q	Marginal gain
22	NA	Glioblastoma	N	NA	Yes	Exon 13, homozygous R521K	6+ *EGFR*
23	NA	Glioblastoma	N	NA	Yes	Exon 13, heterozygous R521K	1+ *EGFR*
24	NA	Glioblastoma	N	NA	Yes	ND	ND
25	NA	Glioblastoma	N	NA	Yes	ND	ND
26	NA	Anaplastic mixed glioma	N	NA	Yes	ND	ND
27	NA	Anaplastic astrocytoma	N	NA	Yes	ND	ND
28	NA	Anaplastic astrocytoma	N	NA	Yes	ND	ND
29	NA	Glioblastoma	N	NA	Yes	ND	ND
30	NA	Glioblastoma	N	NA	Yes	ND	ND
31	NA	Glioblastoma	N	NA	Yes	ND	ND
32	NA	Anaplastic mixed glioma	N	NA	Yes	ND	ND
33	NA	Anaplastic mixed glioma	N	NA	Yes	ND	ND

NOTE: Tumor characteristics, treatment, erlotinib/gefitinib sensitivity, and results. Three sets of paired tumors (1 and 9, 2 and 10, and 3 and 11) were resected from the three patients before and during treatment with erlotinib/gefitinib, respectively.
Abbreviations: NA, not applicable; ND, not done.

serum albumin standards. Western blot detection was done using chemiluminescence (Amersham Pharmacia, Pittsburg, PA) with the following antibodies: anti-pEGFR (Tyr^{1068}) 1:250, anti-total EGFR 1:2,000 (Cell Signaling Technology, Beverly, MA), anti-pAKT (Ser^{473}) 1:1,000 (Cell Signaling Technology), anti-pERK (Thr^{202}/Tyr^{204}) 1:1,000 (Cell Signaling Technology), anti–glyceraldehyde-3-phosphate dehydrogenase 1:2,000 (Upstate, Chicago, IL), horseradish peroxidase–conjugated anti-rabbit Ig 1:1,000 (Amersham Pharmacia), and horseradish peroxidase–conjugated anti-mouse Ig 1:2,000 (Roche). Anti-pEGFR (Tyr^{1068}) antibodies were used because $pTyr^{1068}$ is a reasonable indicator of EGFR autophosphorylation (14, 15).

Pharmacokinetic analysis. For a subset of patients undergoing surgery as part of NABTC trial 01-03, a separate aliquot of tissue was collected for pharmacokinetic analysis following 7 days of erlotinib. Blood was also drawn at the time of surgery and centrifuged within 60 minutes of collection. Tissue (snap frozen in liquid nitrogen at the time of collection) and the simultaneously collected plasma were stored at or below −20°C until analysis. The tissue was weighed and homogenized in 1 mL high-performance liquid chromatography analytic-grade methanol. Concentrations of erlotinib and its *O*-demethylated active metabolite (OSI-420) in plasma and tumor tissue were analyzed using a validated liquid chromatography-mass spectrometry method developed by MDS Pharma Services (Saint-Laurent, Quebec, Canada). Analytic-grade erlotinib and OSI-420 and the internal standard (CP-396,059) were obtained from OSI Pharmaceuticals (Boulder, CO).

Erlotinib and OSI-420 were isolated from plasma and homogenized tissue by liquid/liquid extraction. Briefly, 900 μL plasma (tissue) was added to 100 μL internal standards (500 ng/mL) and vortexed followed by the addition of 4 mL *t*-butyl methyl ether. After circular rotation for 15 minutes at high speed, the samples were centrifuged (3,000 rpm) at 25°C for 5 minutes. The samples were flash frozen and the organic layer was evaporated to dryness under a gentle stream of nitrogen in a 35°C water bath. The dry residue was reconstituted with 200 μL mobile phase and vortexed for 10 seconds. A 20-μL sample was autoinjected at room temperature onto a high-performance liquid chromatography system (HP Series II 1090 high-performance liquid chromatography system, Hewlett Packard, Palo Alto, CA). The mobile phase consisted of 70% methanol:30% ammonium formate (10 mmol/L; pH 4.8) pumped at a flow rate of 0.5 mL/min. Separation of erlotinib and OSI-420 was accomplished using a Waters Symmetry C18 column (50 × 4.6 mm, 3.5 μm; Waters, Milford, MA) preceded by a solvent filter and Waters (2.6 × 10 mm) cartridge guard column. Mass spectrometric detection was done by a Finnigan LCQ spectrometer (San Jose, CA) equipped with an atmospheric pressure chemical ionization probe. The mass spectrometric settings were vaporized temperature 450°C, sheath gas (N_2) flow rate 62 arb, current 5.0 μA, voltage 0.01 kV, capillary temperature 150°C, and capillary voltage 22.0 kV.

In the tandem mass spectrometry mode, the collision energy was 41%. For peak identification, full-scan mass spectra were acquired in the positive ion mode. The tandem mass spectrometry scan range was 90 to 450. Selected ion monitoring was used for the determination of the ammonium adducts [$M + NH_4$] and the compound's respective fragment ion: erlotinib (394.5→278.0 *m/z*), OSI-420 (380.3→278.0 *m/z*), and CP-396,059 (408.4→292.0 *m/z*).

Data acquisition and integration of the chromatograms were done using Xcaliber LCQ program (Finnigan). The chromatographic data were analyzed by linear least-squares regression with a weighting of $1/x^2$ generating a 9- and 7-point calibration curve of area ratios for erlotinib and OSI-420, respectively. The calibration curves were linear ($R^2 > 0.99$) over the range of 1.0 to 3,000 ng/mL for erlotinib and 1.0 to 1,000 ng/mL for OSI-420, respectively. The slope of 15 separate calibration curves used in the analysis of samples over a 2-year span ranged from 0.017 to 0.021 and from 0.006 to 0.010 with mean ± SD values of 0.02 ± 0.001 and 0.009 ± 0.002 for erlotinib and OSI-420, respectively.

Samples were repeated if the independent quality control samples are at the low (3.0 ng/mL, erlotinib/OSI-420) exceeded the theoretical value by 20% and the medium (400 mg/mL erlotinib/150 ng/mL OSI-420) or high (2,400 ng/mL erlotinib/800 ng/mL OSI-420) quality control by 15%. Of the 31 analytic runs done, only 2 of the duplicate quality controls failed. The interday precision for erlotinib/OSI-420 was 8.30%/10.66%, 5.47%/6.98%, and 5.85%/8.31% for the low, medium, and high quality-control samples, respectively.

The patients who underwent surgical resection during gefitinib treatment described in this study did not participate in the pharmacokinetic analysis of tissue for NABTC trial 00-01.

Epidermal growth factor receptor *gene sequencing.* Tumor genomic DNA was isolated from fresh-frozen brain tumors by digestion in DNA isolation mix [50 mmol/L Tris-HCl (pH 8), 100 mmol/L EDTA, 100 mmol/L NaCl, 1% SDS, proteinase K] overnight at 55°C. After addition of RNase A for 1 hour at 37°C, samples were serially extracted with phenol, phenol/chloroform (1:1), and phenol/chloroform/isoamyl alcohol (25:24:1). After isopropanol precipitation, samples were washed in 70% ethanol, air-dried, resuspended in water, and quantified using a spectrophotometer. If frozen tumor was unavailable, paraffin-embedded sections were used. Both deparaffinization (if required) and PCR amplification, including primer sequences, were done as described previously (15). About 90% of the coding region of EGFR (exons 2-28) was successfully sequenced in all tumors analyzed, except one case in which technical limitations resulting from the quality of the DNA extracted from archival paraffinized tumor precluded sequencing of exons beyond 18 to 21 (lung signature region).

Array-based comparative genomic hybridization. Genomic DNA extracted from tumors was analyzed for chromosome alterations affecting not only *EGFR* but also the entire genome. We used Roswell Park Cancer Institute custom comparative genomic hybridization (CGH) arrays spotted with Roswell Park Cancer Institute-11 bacterial artificial chromosomes (BAC) as described previously (16). Verification and use

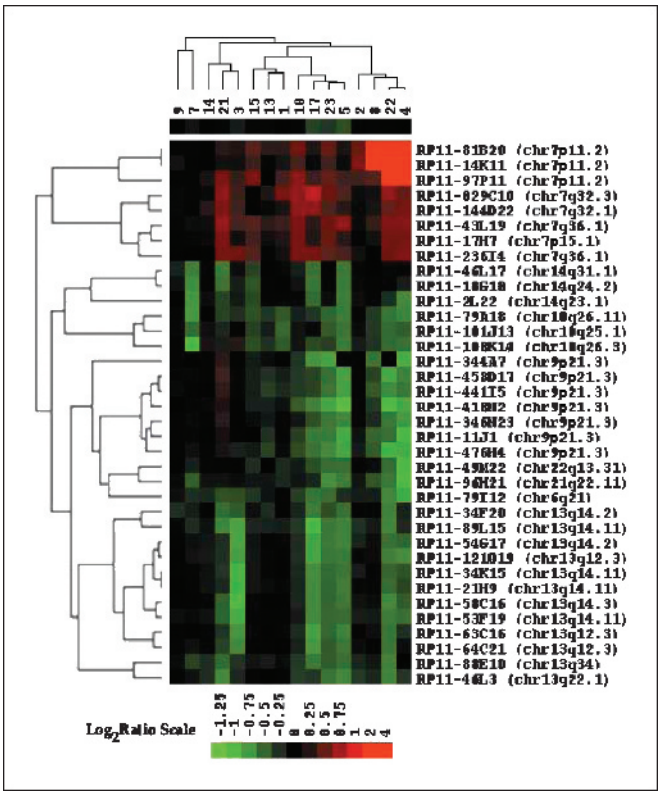

Fig. 2. Two-way hierarchical clustering of aCGH data. Complete linkage clustering of aCGH data from 16 malignant brain tumor samples is shown in the TreeView format. The data are clustered both as tumor groupings (*X axis*) and BAC groupings (*Y axis*). The intensity of *red signal* (amplification) or *green signal* (deletion) is relative to the $\log_2$ ratio (shown in Supplementary Table S1) of a particular BAC for each tumor shown.

of these BACs for array-based CGH (aCGH) has also been reported elsewhere (17, 18). Briefly, the Roswell Park Cancer Institute array contains ~6,000 Roswell Park Cancer Institute-11 BAC clones that provide an average resolution across the genome of 420 kb. BACs were printed in triplicate on amino-silanated glass slides (Schott Nexterion, type A) using a MicroGrid II TAS arrayer (Apogent Discoveries, Hudson, NH) to generate an array of roughly 18,000 elements. Genomic pooled normal control DNA and tumor DNA were fluorescently labeled by random priming and hybridized as described previously (16). Hybridizations of normal and tumor DNA were done as sex-mismatches to provide an internal hybridization control for chromosome X and Y copy number differences. The hybridized slides were scanned using an Affymetrix 428 scanner to generate high-resolution (10 μm) images for both Cy3 and Cy5 channels, and image analysis was done using ImaGene (version 4.1) software (BioDiscovery, Inc., El Segundo, CA). Mapping information was added for each BAC using the National Center for Biotechnology Information July 2003 build (http://genome.ucsc.edu/cgi-bin/hgGateway?org=human), and to the best of our knowledge, clones with ambiguous assignments in the databases were removed.

***Hierarchical cluster analysis and* in silico *mapping*.** The $\log_2$ values of ~5,500 BACs that mapped to autosomal regions of the genome for all 12 tumors were used for hierarchical clustering. The Laboratory of DNA Information Analysis Cluster 3.0 program (http://bonsai.ims.u-tokyo.ac.jp/~mdehoon/software/cluster/) was used to both filter and cluster the aCGH data (19). An *a priori* filter was used to exclude BACs with $\log_2$ ratios between −0.5 and +0.5 in <25% of the tumors analyzed. In practical terms, a $\log_2$ ratio of −0.5 for a genomic region defined by a BAC is equivalent to a heterozygous deletion of a diploid population of cells. In the same respect, each 0.5 increase in the $\log_2$ ratio suggests gain of an additional copy of that region defined by a BAC. Filtered data were hierarchically clustered using the complete linkage setting of the Cluster 3.0 program, and clustered data were viewed using EisenLab TreeView software (http://rana.lbl.gov/EisenSoftware.htm). This method of filtering and clustering allows for the detection of minimal regions of amplification and deletion, thus facilitating the identification of potential target genes. A SD cutoff rule method described previously (20) was also employed to attain independent statistical confirmation of the BACs represented in the cluster analysis. Essentially, the SD cutoff rule is a conservative algorithm that sets a strict threshold to exclude both infrequent and marginal (degree of change < 1 SD from the mean) amplifications/deletion events. Therefore, BACs identified in this report include only those meeting numerous criteria for significance, including frequency and amplitude by both supervised clustering and SD cutoff rule methods.

The genomic position of each BAC is defined as the region containing the BAC as well as the flanking sequence extending from the 3′ end of the adjacent upstream BAC to the 5′ end of the closest downstream BAC. The BACs used for aCGH were mapped using the National Center for Biotechnology Information July 2003 build, and the genomic positions of regions of amplification and deletion were converted to the National Center for Biotechnology Information May 2004 build using the University of California-Santa Cruz Build Converter Browser (http://genome.ucsc.edu/cgi-bin/hgGateway). Genes were identified using both University of California-Santa Cruz and National Center for Biotechnology Information Map Viewer Browser (http://www.ncbi.nlm.nih.gov/mapview/).

Results

Effects of erlotinib and gefitinib on epidermal growth factor receptor activity, expression, and signaling. To determine whether erlotinib/gefitinib inhibited EGFR activity *in vivo*, the pEGFR levels in tissue resected during erlotinib/gefitinib were compared with the levels in erlotinib/gefitinib unexposed tissue by Western blot. In three patients, tissue was resected both before and during treatment with erlotinib or gefitinib. In the first case (tumor 1 versus tumor 9), the level of pEGFR actually increased substantially during treatment with erlotinib (Fig. 1B), although the levels of downstream signaling through pERK and pAKT were markedly reduced. In the second case (tumor 2 versus tumor 10), pEGFR diminished slightly during treatment with gefitinib, but downstream signaling through pERK and pAKT was unchanged and moderately increased, respectively (Fig. 1B). In the third case, EGFR activity was reduced after exposure to gefitinib (tumor 3 versus tumor 11), but signaling through pERK and pAKT slightly increased and decreased, respectively (Fig. 1B).

There was a wide range of pEGFR levels among all 12 tumors resected during erlotinib or gefitinib (Fig. 1C), and this range did not differ substantially from the range observed among the 12 erlotinib/gefitinib unexposed controls (data from 6 representative controls shown; Fig. 1C). The range of pERK and pAKT levels among the erlotinib/gefitinib–exposed tumors and unexposed controls also did not differ substantially (Fig. 1C). These results suggest that erlotinib and gefitinib did not effectively inhibit either EGFR phosphorylation or signaling in these tumors as a group.

Although the range of pEGFR, pERK, and pAKT among erlotinib/gefitinib–exposed and unexposed tumors overlapped, there were several tumors resected during erlotinib/gefitinib therapy with either low (Fig. 1C; tumors 15 and 19) or high (Fig. 1C; tumors 9, 12, 14, and 16) pEGFR levels. However, there was no obvious association between erlotinib/gefitinib sensitivity (as defined in Materials and Methods) and effects on EGFR activity, EGFR expression, or activation of downstream signaling through RAS/MAPK or PI3K/AKT in these tumors (Fig. 1C). Unfortunately, tissue was not resected during treatment of the patient with the complete and sustained radiographic response to erlotinib; therefore, it is unknown whether erlotinib significantly affected EGFR phosphorylation or signaling in this tumor and whether any such effects were related to control of tumor growth.

We also analyzed pharmacokinetic data to determine drug penetration into tumor tissue. The steady-state trough concentrations of erlotinib and the active metabolite OSI-420 in tumor were 6% to 8% and 5% to 11%, respectively, of the concentrations in plasma drawn during the tumor surgery in four available cases (12, 15, 19, 20). As above, there was no consistent association of erlotinib treatment with either clinical outcome or EGFR signaling effects in these cases. In another case (9), erlotinib and OSI-420 were present in the tumor tissue at 50% and 54% of the concentration in plasma, respectively, suggesting a higher tissue penetration. Surprisingly, this was the case with a marked increase in pEGFR during erlotinib treatment. However, pharmacokinetic results from this case and from another (14) with both high pEGFR during treatment and possibly high drug penetration (erlotinib and OSI-420 present in tumor at 19% and 28%, respectively, of the concentration in plasma) are suspect because the tissue aliquots (different than the aliquots analyzed for EGFR activity) were likely contaminated by a large blood clot. In summary, the pharmacokinetic data suggest that drug penetration was too low in the cases analyzed to consistently achieve inhibition of EGFR phosphorylation, and in one case with higher penetration (if not artifactual), EGFR phosphorylation actually increased during treatment.

Aliquots of the tumors analyzed for EGFR signaling changes during gefitinib treatment (10, 11, 16) were not available for

pharmacokinetic analysis. However, analysis of analogous tumors obtained from other patients receiving gefitinib through NABTC trial 00-01 ($n = 2$) revealed that the 24-hour trough tissue-to-plasma ratio was 221% to 370%. This suggests that gefitinib is sequestered in, rather than excluded, from glioma tissue. Applying these data to the cases studied for effects on EGFR activity, it is likely that the dose of gefitinib given was sufficient to slightly or moderately inhibit EGFR phosphorylation in the two cases in which tissue resected both before and during gefitinib was available for comparison (2 versus 10 and 3 versus 11; Fig. 1B).

Combining results from both erlotinib and gefitinib exposed tissue, it is of potential interest that pAKT was reduced during treatment in two tumors that were erlotinib/gefitinib sensitive (Fig. 1B, tumor 1 versus tumor 9 and tumor 3 versus tumor 11) and higher in one insensitive tumor (Fig. 1B, tumor 2 versus 10) despite the lack of consistent effects on pEGFR and relatively low erlotinib penetration. However, this pattern was not clearly evident in the other tumors resected during treatment (Fig. 1C), and the interpretation is also limited by the number of cases with both pretreatment and during treatment specimens available for comparison. Therefore, the clinical relevance of the decrease in pEGFR during gefitinib (Fig. 1B) as well as the changes in pERK and/or pAKT remain unclear.

Epidermal growth factor receptor *gene sequencing*. It was reported recently that several mutations in *EGFR* exons 18 to 21 are associated with sensitivity of non–small cell lung cancer to erlotinib and gefitinib (15, 21, 22). In light of these results, we first screened genomic DNA from 16 of the gliomas for the lung signature mutations (tumors 1-2, 4-10, 13-15, 17, and 21-23). Although two single nucleotide alterations without a corresponding amino acid change were observed (data not shown), we did not identify any of the mutations reported in non–small cell lung cancer. Therefore, we sequenced the remainder of the *EGFR* coding sequence in an attempt to identify other mutations, including any that were associated with sensitivity to erlotinib/gefitinib. Ten single nucleotide alterations that did not induce an amino acid change were observed (data not shown). There were also missense mutations in exons 6, 13, and 17 (1 each). In tumor 8, heterozygous C219Y (exon 6; 656 G→A) was observed. This mutation was not found in any other tumor from patients either treated or untreated with gefitinib or erlotinib. In tumor 21, heterozygous R675Q (exon 17; 2,024 G→A) was observed. This mutation was similarly not observed in any other tumor from patients either treated or untreated with gefitinib or erlotinib. Three tumors exhibited heterozygous (13, 14) or homozygous (15) R521K (exon 13; 1,562 G→A) mutations. Notably, this mutation was also observed in both tumors (22, 23) from a patient that was not treated with gefitinib or erlotinib as well as in several brain metastases from non–small cell lung cancer (data not shown). There were no large homozygous deletions that have been reported by others in malignant gliomas (7, 9), such as that of exons 2 to 7 in the mutant form *EGFRvIII*. Although heterozygous *EGFRvIII* and similar mutations were not observed, exonic resequencing is not the optimal technique to detect multiexon heterozygous deletions. As none of these changes was clearly associated with sensitivity to erlotinib or gefitinib, sequencing of *EGFR* was not pursued in the remaining tumors.

Array-based comparative genomic hybridization. In addition to assays of EGFR activity and signaling, we also examined chromosome 7p11.2 (containing the *EGFR* gene) for amplifications or deletions using aCGH. Three tumors (4, 8, 22) exhibited genomic amplification of at least six copies of the Chr7:54860933-55049239 region identified by three contiguous BACs (RP11-14K11, RP11-81B20, and RP11-97P11; Fig. 2). Tumors with high copy *EGFR* gene amplification determined by aCGH analysis also exhibited high total EGFR protein expression when assayed by Western blot [e.g., tumors 4 and 8 (Fig. 1B) and tumor 22 (data not shown)] serving as an internal control validating our results. However, there was no association between erlotinib sensitivity and *EGFR* amplification.

Expanding the analysis beyond *EGFR*, supervised clustering of aCGH identified genetic alterations consistent with malignant brain tumors, such as deletions of the *p16* gene (Chr9:21957751-21984357) and loss of chromosome 10q23-26 in six (4, 5, 8, 17, 22, and 23) and seven (1, 4, 5, 7, 15, 22, and 23) of the tumors, respectively (Table 2). Although this analysis focused exclusively on the most frequent changes, events unique to this population of tumors included amplifications of *MYCN* (Chr2:15,250,313-18,548,231) and *GLI1* (Chr12:55,804,692-57,375,460) in tumors 17 and 21, respectively.

In addition to expected losses and gains, we identified recurrent losses of entire copies of chromosomes 13, 14, and 22 as well as loss of a single BAC (RP11-96H21) on chromosome 21. In addition, a region of 7q36.1 containing two contiguous BACs (RP11-236I4 and RP11-43L19) was amplified in tumors 3-5, 10, 17, and 21-23. Amplification of this region may be due to gain of a complete copy of chromosome 7, but in at least one specimen (tumor 17), amplification of this region (Chr7:150340429-152159943) occurred without amplification of *EGFR*. Although there are 23 known genes mapped to this region of 7q, at least one, *Ras homologue enriched in brain* (*RHEB*), may contribute to the malignant phenotype. Similarly, loss of two contiguous BACs on chromosome 13 represent a 437-kb region containing six genes, one of which, *forkhead box O1A* (*FOXO1A*), is a known tumor suppressor. Both RHEB and forkhead transcription factors are involved in PI3K/AKT signaling, suggesting that aCGH may be used to identify candidate genes within specific pathways involved in malignant brain tumors.

In addition to RHEB and FOXO1A, deletion of chromosome 14 was prominent in five tumors (5, 7, 15, 17, and 21), and partial loss (Chr14:57910104-58786387, BAC RP11-2L22) occurred in one tumor (tumor 4). This region of chromosome 14 contains 11 known genes, one of which, *disheveled associated activator of morphogenesis 1* (*DAAM1*), is the best characterized and has a known role in the Wnt signaling pathway (23). Other highlighted BACs on chromosome 14 include those containing the gene *MAX*, which is involved in MYC signaling, and *PTPN21*, which encodes a protein tyrosine phosphatase.

We also identified deletions of chromosomes 6 (tumors 4, 17, 22, and 23), 21 (tumors 4, 5, 7, 8, 22, and 23), and 22 (tumors 4, 5, 17, 22, and 23) that have not been reported previously in brain tumors. Although there was no evidence of an association between deletion or amplification events and sensitivity to erlotinib, the consistency of chromosomal alterations identified in our tumor samples suggests that genes mapped to these regions may be worthy of further study in gliomas.

Discussion

To fulfill the primary molecular aims of NABTC trials 01-03 and 00-01, which involved erlotinib and gefitinib for recurrent or progressive malignant gliomas, 21 available gliomas were analyzed to determine the molecular consequences of EGFR inhibitor treatment *in vivo*. Comparison of tumor resected during erlotinib or gefitinib with control tissue did not show a consistent effect on EGFR phosphorylation or downstream signaling (Fig. 1B and C). Furthermore, reduced EGFR activity and downstream signaling was also not related to erlotinib/gefitinib sensitivity. Although the strength of our conclusions is limited by the small number of samples available for analysis, other studies have yielded similar results. For example, pEGFR reduction in breast tumors following treatment with gefitinib did not correlate with response (24). Similarly, amplification of chromosome 7p (containing the *EGFR* gene) was unrelated to erlotinib sensitivity. Others have also reported no relationship between *EGFR* gene amplification or protein expression and sensitivity of breast, lung, or brain tumors to EGFR inhibitors (25–30).

Taken together, these data suggest that erlotinib and gefitinib did not have a consistent effect on EGFR phosphorylation in the gliomas analyzed. Although a *molecularly effective dose* of erlotinib/gefitinib (required to achieve consistent pathway inhibition) has not been determined and may differ from a maximally tolerated dose, these data suggest that the concentration of erlotinib in tumor tissue relative to simultaneously collected plasma was too low (steady-state trough levels of ~10% or less for both erlotinib and its active metabolite) to consistently reduce pEGFR, and it is possible that erlotinib was markedly underdosed in this study. In fact, the tissue with the highest penetration by drug actually exhibited a marked increase rather than decrease in EGFR phosphorylation, despite clinical sensitivity to erlotinib, although the high drug concentration in that sample could be artifactual as described above. Of note, the pharmacokinetic results are also limited by the availability of only one tissue specimen per patient representing a trough level 24 hours after dosing. It is possible that levels at time points earlier than 24 hours after drug exposure would have been higher. By contrast, the mean gefitinib concentration in two tumors from other patients treated through NABTC trial 00-01 (not assayed for EGFR signaling changes) was almost triple the concentration in plasma. This may explain the reductions in pEGFR seen in two cases (2 versus 10 and 3 versus 11), although pEGFR remained relatively high in a third case (16).

Although there was no consistent effect of erlotinib or gefitinib on EGFR activity, expression, or signaling and no

Table 2. Results of aCGH analysis

Tumors	Genomic position	BAC(s)	Event	No. gene(s)	Representative gene(s) symbol and description
4, 17, 22, and 23	Chr6:113168055-113666837	RP11-79I12	Loss	2	*LOC389424*, cell cycle protein p38-2G4 homologue; *LOC442250*, similar to SOCS-5
4, 10, 21, and 22	Chr7:27746109-28559975	RP11-17H7	Gain	4	*CREB5, cyclic AMP – responsive element binding protein 5*
2, 4, 8, 10, 15, 22,	Chr7:53864617-55274089	RP11-14K11 RP11-81B20 RP11-97P11	Amplification	8	*EGFR, epidermal growth factor receptor*
4, 10, 17, and 21	Chr7:127774792-127909559	RP11-144D22	Gain	5	*LOC284701*; *LOC402483*, novel protein similar to septin; *LOC346653*
1, 10, 17, and 21-23	Chr7:129745678-132155850	RP11-829C10	Gain	15	*MKLN1*, *muskelin 1*; *PLXNA4, plexin A4*
3-5, 10, 17, and 21-23	Chr7:150340429-152159943	RP11-236I4 RP11-43L19	Gain	23	*PRKAG2, protein kinase, AMP activated, $\gamma 2$*; *RHEB, Ras homologue enriched in brain*
4, 5, 8, 17, 22, and 23	Chr9:21588345-23900188	RP11-344A7 RP11-441I5 RP11-458D17 RP11-11J1 RP11-476H4 RP11-346N23 RP11-418N2	Loss	10	*CDKN2A, cyclin-dependent kinase inhibitor 2A,* p16; *CDKN2B, cyclin-dependent kinase inhibitor 2B*, p16
1, 4, 5, 7, 15, 22, and 23	Chr10:106023284-106201712	RP11-101J13	Loss	4	*GSTO2, glutathione S-transferase $\omega 2$*; *C10orf80*; *KIAA1754*; *LOC387710*
1, 4, 5, 7, 15, 22, and 23	Chr10:119134985-120589963	RP11-79A18	Loss	7	*CASC2, cancer susceptibility candidate 2*
1, 4, 5, 7, 15, 22, and 23	Chr10:135111183-135150439	RP11-108K14	Loss	3	*Sprn, shadow of prion protein*; *LOC399832*

(*Continued on the following page*)

consistent association with clinical outcome (Fig. 1C), it is interesting to note that pAKT was reduced during treatment in two sensitive tumors and increased in one insensitive tumor (Fig. 1B). If confirmed by analysis of more tumors, this could suggest that the PI3K/AKT cascade deserves particular focus during treatment of gliomas with EGFR inhibitors and may be a more important indicator of EGFR inhibition than EGFR phosphorylation status. In fact, there has been conflicting data regarding the importance of RAS/MAPK and PI3K/AKT activity in relationship to sensitivity to upstream inhibition of EGFR (31–36). It is also possible that erlotinib and gefitinib may affect other receptor tyrosine kinases or other signaling cascades not studied in this analysis, as the number of tyrosine kinases studied for activity is limited (37).

It is also notable that the level of phosphorylation mirrored the total EGFR expression in all three cases where both pre–erlotinib/gefitinib and during erlotinib/gefitinib–exposed tissue were analyzed. In one case (1 versus 9; Fig. 1B), it is plausible that the downstream effects of EGFR (pERK and pAKT) were inhibited by erlotinib and the increase in total EGFR protein expression (and pEGFR) resulted from stimulation of a feedback loop following the block in downstream signaling. Along the same lines, the reduction in pEGFR during exposure to gefitinib (2 versus 10 and 3 versus 11; Fig. 1B) could simply reflect the reduction of total EGFR protein expression without biologically relevant change in the phospho/total ratio or effect on downstream signaling.

In addition, mutations in *EGFR* exons 18 to 21 that predict sensitivity of lung cancer to erlotinib (15) and gefitinib (15, 21, 22) were not present in the malignant gliomas we analyzed. These results both confirm and extend the data of others who observed no amino acid altering mutations in the kinase domain of 9 glioblastomas that were sensitive to gefitinib (38) and 63 glioblastomas of unreported sensitivity (21, 39). In erlotinib/gefitinib–sensitive gliomas resected during erlotinib/gefitinib therapy, it is theoretically possible that the sensitizing mutations were present in a subpopulation of tumor cells that were selectively killed. However, we find this unlikely as none of the pre–erlotinib/gefitinib or erlotinib/gefitinib unexposed tumors exhibited the mutations. Gliomas and lung cancers likely represent distinct molecular entities despite the presence of *EGFR* gene amplification and constitutively activating mutations common to both cancer types.

We did observe missense mutations in *EGFR* exons beyond the 18 to 21 region. One such point mutation (R521K; exon 13; 1,562 G→A) is relatively conservative as both R and K are positively charged amino acids with similar side chains. Therefore, this mutation may not have functional relevance

Table 2. Results of aCGH analysis (Cont'd)

Tumors	Genomic position	BAC(s)	Event	No. gene(s)	Representative gene(s) symbol and description
3-5, 17, and 21-23	Chr13:29592937-30684939	RP11-121O19 RP11-64C21 RP11-63C16	Loss	13	*HMGB1, high-mobility group box 1*; *KATNAL1, katanin p60 subunit A-like 1*; *LOC387917*; *FLJ14834*
3-5, 17, and 21-23	Chr13:39103232-40367433	RP11-53F19 RP11-89L15	Loss	6	*COG6, component of oligomeric Golgi complex 6*; *FOXO1A, forkhead box O1A*
3-5, 17, and 21-23	Chr13:41593291-42577676	RP11-21H9 RP11-34K15	Loss	8	*DGKH, diacylglycerol kinase*; *AKAP11, A kinase (PRKA) anchor protein 11*; *TNFSF11, tumor necrosis factor (ligand) superfamily member 11*; *EPSTI1, epithelial stromal interaction 1 (breast)*
4, 5, 17, and 21-23	Chr13:48242971-50898649	RP11-54G17 RP11-34F20 RP11-58C16	Loss	22	*DLEU1-2, Losseted in lymphocytic leukemia, 1 and 2*; *MLNR, motilin receptor*; *FNDC3, fibronectin type III domain 3*
4, 5, 7, 15, 17, and 21	Chr14:57910104-58786387	RP11-2L22	Loss	11	*DACT1, dapper homologue 1, antagonist of* β-catenin; *DAAM1, dishevelled associated activator of morphogenesis 1*
5, 7, 15, 17, and 21	Chr14:69440807-70531028	RP11-18G18	Loss	14	*MAP3K9, MAPK kinase kinase 9*
5, 7, 15, 17, and 21	Chr14:77626345-79602555	RP11-46L17	Loss	2	*NRXN3, neurexin 3*; *LOC388001*
4, 5, 7, 8, 22, and 23	Chr21:29921601-31102834	RP11-96H21	Loss	33	*KRTAP, keratin-associated proteins*; *CLDN8, claudin 8*
4, 5, 17, 22, and 23	Chr22:31113067-31577786	RP11-70F2	Loss	5	*SYN3, synapsin III*; *TIMP3, tissue inhibitor of metalloproteinase*

NOTE: Defining regions frequently amplified or deleted in malignant brain tumors. A total of 36 BACs corresponding to 19 discrete loci were identified by aCGH as either gained or lost in at least 25% of the brain tumors analyzed. Contiguous BACs are shown with a vertical line, and the genomic position for each BAC(s) incorporates the genomic distance between BACs immediately proximal and distal to the known region of amplification or deletion. Each locus is identified as being a region of loss, gain (increase in one or two copies generally of an entire chromosome or chromosomal arm), or amplification (multiple copies of a particular locus). The total number of genes that map to each region is also shown with examples of either known or potential target genes.

and rather represent a polymorphism, a conclusion further supported by the identification of this change in other gliomas as well as in brain metastases from non–small cell lung cancer. Another change (C219Y; exon 6; 656 G→A) was not detected in tumors from other patients treated or untreated with gefitinib or erlotinib. The importance of this alteration is unclear. It should also be noted that *EGFR* mutations are typically observed only in gliomas with *EGFR* gene amplifications (9). Therefore, one limitation of our analysis for *EGFR* gene mutations was that amplified *EGFR* (at least one extra copy) was observed in only seven of the tumors analyzed (Table 1), and relatively rare mutations could be missed in tumors without amplified *EGFR*. We also did not identify homozygous *EGFRvIII* in any of the tumors in which *EGFR* was sequenced. However, others have reported that EGFRvIII expression does not correlate with sensitivity of malignant gliomas to gefitinib (29).

Finally, the aCGH analysis also did not identify other areas of change in genomic DNA outside the *EGFR* region associated with erlotinib/gefitinib sensitivity. However, while investigating genomic DNA changes beyond *EGFR*, we identified several areas that were consistently amplified or deleted. The genes contained within these areas involve varied aspects of cancer and cellular biology (Table 2). Some of these are already identified as important in glioma biology, but others are novel. Further investigation of these regions may improve our understanding of malignant brain tumors.

In summary, we analyzed malignant gliomas resected during treatment with the EGFR inhibitors erlotinib or gefitinib for changes in EGFR expression, activity, or signaling *in vivo*. No consistent effects were observed. However, nonsustained stable disease was included in the definition of clinical sensitivity to erlotinib/gefitinib for this analysis, and in the only case with an objective response (complete disappearance of visible tumor), tissue was not resected during exposure to erlotinib precluding analysis of either EGFR signaling or drug penetration during treatment. We also did not identify DNA alterations either in *EGFR* or elsewhere that associated with tumor sensitivity to erlotinib/gefitinib. The molecular features associated with erlotinib/gefitinib therapy for gliomas remain unclear.

Appendix

The NABTC is dedicated to the development and conduct of innovative clinical trials that will ultimately result in a cure for patients with malignant brain tumors. More information about the NABTC is available by visiting http://www.nabtc.org or by calling 713-792-8519.

Tissue was available for analysis from patients treated at four participating NABTC sites: Memorial Sloan Kettering Cancer Center, Dana-Farber Cancer Institute, University of California-San Francisco, and University of Texas M.D. Anderson Cancer Center. As results reported here are restricted to the analysis of available tissue from these centers, authorship was limited to investigators from these centers and to the multicenter principal investigators. Clinical results will be reported separately, and we recognize and appreciate the contribution to the clinical data made by the site principal investigators for the other NABTC centers, including Drs. Timothy F. Cloughesy (University of California-Los Angeles), Howard A. Fine (Neuro-Oncology Branch, National Cancer Institute, NIH), and Minesh Mehta (University of Wisconsin Hospital and Clinics) and their many colleagues. NABTC 01-03 and 00-01 would not have been possible without the invaluable assistance of multiple research staff assistants, nurses, and data managers.

Acknowledgments

We thank Judy Lampron for key editorial assistance in article preparation, and Bill Carey for administrative assistance, Maria Salpietro for assistance with the tumor bank, Jennifer Doherty (Memorial Sloan Kettering Cancer Center) for DNA extraction and PCR for *EGFR* gene analysis, and Dr. Harold Varmus who collaborated on the *EGFR* gene sequencing and gave critical review of the manuscript.

References

1. DeAngelis LM. Brain tumors. N Engl J Med 2001; 344:114–23.
2. Mischel PS, Cloughesy TF. Targeted molecular therapy of GBM. Brain Pathol 2003;13:52–61.
3. Wong AJ, Bigner SH, Bigner DD, Kinzler KW, Hamilton SR, Vogelstein B. Increased expression of the epidermal growth factor receptor gene in malignant gliomas is invariably associated with gene amplification. Proc Natl Acad Sci U S A 1987;84: 6899–903.
4. Kleihues P, Ohgaki H. Primary and secondary glioblastomas: from concept to clinical diagnosis. Neuro-oncol 1999;1:44–51.
5. Schlegel J, Stumm G, Brandle K, et al. Amplification and differential expression of members of the erbB-gene family in human glioblastoma. J Neurooncol 1994;22:201–7.
6. Humphrey PA, Wong AJ, Vogelstein B, et al. Anti-synthetic peptide antibody reacting at the fusion junction of deletion-mutant epidermal growth factor receptors in human glioblastoma. Proc Natl Acad Sci U S A 1990;87:4207–11.
7. Kuan CT, Wikstrand CJ, Bigner DD. EGF mutant receptor vIII as a molecular target in cancer therapy. Endocr Relat Cancer 2001;8:83–96.
8. Wikstrand CJ, Hale LP, Batra SK, et al. Monoclonal antibodies against EGFRvIII are tumor specific and react with breast and lung carcinomas and malignant gliomas. Cancer Res 1995;55:3140–8.
9. Frederick L, Wang XY, Eley G, James CD. Diversity and frequency of epidermal growth factor receptor mutations in human glioblastomas. Cancer Res 2000; 60:1383–7.
10. Schlessinger J. Ligand-induced, receptor-mediated dimerization and activation of EGF receptor. Cell 2002;110:669–72.
11. Raizer JJ, Abrey LE, Wen P, et al. A phase II trial of erlotinib (OSI-774) in patients (pts) with recurrent malignant gliomas (MG) not on EIAEDs [abstract]. J Clin Oncol 2004;22:1502.
12. Lieberman FS, Cloughesy T, Malkin M, et al. Phase I-II study of ZD-1839 for recurrent malignant gliomas and meningiomas progressing after radiation therapy [abstract 421]. J Clin Oncol 2003;22:105.
13. Macdonald DR, Cascino TL, Schold SC, Jr., Cairncross JG. Response criteria for phase II studies of supratentorial malignant glioma. J Clin Oncol 1990; 8:1277–80.
14. Sordella R, Bell DW, Haber DA, Settleman J. Gefitinib-sensitizing EGFR mutations in lung cancer activate anti-apoptotic pathways. Science 2004; 305:1163–7.
15. Pao W, Miller V, Zakowski M, et al. EGF receptor gene mutations are common in lung cancers from "never smokers" and are associated with sensitivity of tumors to gefitinib and erlotinib. Proc Natl Acad Sci U S A 2004;101:13306–11.
16. Cowell JK, Wang YD, Head K, Conroy J, McQuaid D, Nowak NJ. Identification and characterisation of constitutional chromosome abnormalities using arrays of bacterial artificial chromosomes. Br J Cancer 2004; 90:860–5.
17. Cheung VG, Nowak N, Jang W, et al. Integration of cytogenetic landmarks into the draft sequence of the human genome. Nature 2001;409:953–8.
18. Snijders AM, Nowak N, Segraves R, et al. Assembly of microarrays for genome-wide measurement of DNA copy number. Nat Genet 2001;29:263–4.
19. de Hoon MJ, Imoto S, Nolan J, Miyano S. Open source clustering software. Bioinformatics 2004;20: 1453–4.
20. Rossi MR, Gaile D, Laduca J, et al. Identification of consistent novel submegabase deletions in low-grade oligodendrogliomas using array-based comparative genomic hybridization. Genes Chromosomes Cancer 2005;44:85–96.
21. Lynch TJ, Bell DW, Sordella R, et al. Activating mutations in the epidermal growth factor receptor underlying responsiveness of non-small-cell lung cancer to gefitinib. N Engl J Med 2004;350:2129–39.
22. Paez JG, Janne PA, Lee JC, et al. EGFR mutations in lung cancer: correlation with clinical response to gefitinib therapy. Science 2004;304:1497–500.
23. Habas R, Kato Y, He X. Wnt/Frizzled activation of Rho regulates vertebrate gastrulation and requires a novel Formin homology protein Daam1. Cell 2001; 107:843–54.

24. Baselga J, Albanell J, Ruiz A, et al. Phase II and tumor pharmacodynamic study of gefitinib (ZD1839) in patients with advanced breast cancer [abstract 24]. Proc Am Soc Clin Oncol 2003.

25. Vogelbaum MA, Peerboom G, Stevens G, Barnett G, Brewer C. Phase II trial of the EGFR tyrosine kinase inhibitor erlotinib for single agent therapy of recurrent glioblastoma multiforme: interim results [abstract]. J Clin Oncol 2004;22:1558.

26. Sirotnak FM, Zakowski MF, Miller VA, Scher HI, Kris MG. Efficacy of cytotoxic agents against human tumor xenografts is markedly enhanced by coadministration of ZD1839 (Iressa), an inhibitor of EGFR tyrosine kinase. Clin Cancer Res 2000;6: 4885–92.

27. Bailey LR, Kris M, Wolf M, et al. Tumor EGFR membrane staining is not clinically relevant for predicting response in patients receiving gefitinib ("Iressa," ZD1839) monotherapy for pretreated advanced non-small cell lung cancer: IDEAL1 and 2 [abstract LB-170]. Proc Am Assoc Cancer Res 2003;44:1362.

28. Perez-Soler R, Chachoua A, Huberman M, et al. A phase II trial of epidermal growth factor receptor (EGFR) tyrosine kinase inhibitor OSI-774, following platinum-based chemotherapy, in patients with advanced, EGFR-expressing, non-small cell lung cancer [abstract 1235]. Proc Am Soc Clin Oncol 2001.

29. Rich JN, Reardon DA, Peery T, et al. Phase II trial of gefitinib in recurrent glioblastoma. J Clin Oncol 2004; 22:133–42.

30. Uhm JH, Ballman KV, Giannini C, et al. Phase II study of ZD1839 in patients with newly diagnosed grade 4 astrocytoma [abstract]. J Clin Oncol 2004;22:1505.

31. Cappuzzo F, Magrini E, Ceresoli GL, et al. Akt phosphorylation and gefitinib efficacy in patients with advanced non-small-cell lung cancer. J Natl Cancer Inst 2004;96:1133–41.

32. Pao W, Zakowski M, Cordon-Cardo C, Ben-Porat L, Kris MG, Miller VA. Molecular characteristics of non-small cell lung cancer (NSCLC) patients sensitive to gefitinib [abstract 7025]. J Clin Oncol 2004;22:619.

33. Franklin WA, Chansky K, Gumerlock PH, et al. Association between activation of ErbB pathway genes and survival following gefitinib treatment in advanced BAC (SWOG 0126) [abstract 7019]. J Clin Oncol 2004;22.

34. Janmaat ML, Kruyt FA, Rodriguez JA, Giaccone G. Response to epidermal growth factor receptor inhibitors in non-small cell lung cancer cells: limited antiproliferative effects and absence of apoptosis associated with persistent activity of extracellular signal-regulated kinase or Akt kinase pathways. Clin Cancer Res 2003; 9:2316–26.

35. Stallings-Mann M, Wharen R, Thomas CY. Resistance of glioblastoma cells to an EGFR kinase inhibitor is associated with maintenance of signaling by phosphatidylinositol-3-kinase (PI3K) and constitutive phosphorylation of the Gab1/Gab2 adapter proteins [abstract 72]. Proc Am Soc Clin Oncol 2002.

36. She QB, Solit D, Basso A, Moasser MM. Resistance to gefitinib in PTEN-null HER-overexpressing tumor cells can be overcome through restoration of PTEN function or pharmacologic modulation of constitutive phosphatidylinositol 3′-kinase/Akt pathway signaling. Clin Cancer Res 2003;9:4340–6.

37. Pao W, Miller VA, Kris MG. "Targeting" the epidermal growth factor receptor tyrosine kinase with gefitinib (Iressa) in non-small cell lung cancer (NSCLC). Semin Cancer Biol 2004;14:33–40.

38. Rich JN, Rasheed BK, Yan H. EGFR mutations and sensitivity to gefitinib, comments. N Engl J Med 2004; 351:1260.

39. Barber TD, Vogelstein B, Kinzler KW, Velculescu VE. Somatic mutations of EGFR in colorectal cancers and glioblastomas. N Engl J Med 2004;351:2883.